Velocity Analysis by Focusing Diffractions Simulated from CRS-attributes

G. Garabito (UFRN), W. Söllner (PGS), W. Lima (UFPA), I. G. Oliveira (UFPA)

This paper was prepared for presentation during the 12th International Congress of the Brazilian Geophysical Society held in Rio de Janeiro, Brazil, August 15-18, 2011.

The kinematic attributes of the common-reflection-surface (CRS) stack method have several applications in reflection seismics. These attributes are determined from multi-coverage data by means of optimization strategies based on the coherency measures of the seismic signal. The three CRS-attributes, related to the Normal Incidence Point (NIP) wave and Normal wave, provide important information about the local properties of the reflectors. In particular, the NIP-wave attributes can be used to determine a layered velocity model and gridded smoothed velocity model. In this work, we use the NIP-wave attributes to build an interactive velocity estimation process based on focusing analysis of diffractions simulated in CRS stacked sections. This approach can be applied in time and depth velocity model estimation, and it is validated here using synthetic data of a layered model with dipping and curved interfaces. The results show that this velocity estimation is stable and a reliable approach to obtain geologically consistent velocity models.

Introduction

In 2D, the CRS stack method simulates a zero offset (ZO) stacked section with a high signal-to-noise ratio from multi-coverage seismic data. This data-driven and velocity-independent stacking method provides as byproducts three important kinematic attributes, namely, the emergency angle of the normal ray, β_0, the radius of curvature of the NIP wave, R_{NIP}, and the radius of curvature of the normal wave, R_N.

The CRS-attributes can be determined form prestack data by means of optimization strategies based on the coherency measure of the seismic signal. In 2D, Jager et al., (2001) introduced a multi-step search strategy to determine the CRS attributes. This well-established strategy was modified by Mann (2001) to take into account the conflicting dip events and velocity information in the search process. In order to avoid the use of several steps and improve the accuracy of the parameter estimation, Garabito et al., (2006) introduce a one-step search strategy, where the three CRS parameters are determined simultaneously using the Simulated Annealing (SA) or Very Fast Simulated Annealing (VFSA) global optimization algorithms.

In Biloti et al., (2002) the NIP-wave attributes resulting from the CRS stack were applied to determine a layered depth velocity model. They use an inversion algorithm based on back-propagation of the NIP-wavefront, by employing a modified version of the classical inversion of Hubral and Krey (1980). Also, following the idea of focusing the NIP-wave front, Söllner and Yang, (2002) presented an approach to determine a layered depth velocity model by means of interactive focusing analysis of simulated diffractions in poststack data. In that work the diffraction events are simulated from NMO stacking velocities and ZO reflection slopes. By applying a tomographic inversion of the NIP-wave attributes, Duveneck, (2004) determined a gridded smooth depth velocity model. In general, the inversion methods are not stable. As a consequence the velocity models determined by these methods are not geologically consistent, and as such neither the results obtained by NIP-tomography.

In this work, following the same approach as Söllner and Yang, (2002), we present a CRS stack based velocity model determination from NIP-wave attributes. Using synthetic data of a layered model with curved interfaces, we demonstrate first the focusing of simulated diffractions in depth by applying a poststack depth migration and show secondly how we use simulated diffractions in an interactive velocity estimate process.

THEORETICAL ASPECTS

CRS-Traveltime

The CRS stacking traveltime surface is based on three kinematic wavefront attributes, namely: the emergence angle *beta*$_0$ of the central ray and the two radii of curvature R_{NIP} and R_N, which correspond to the hypothetical NIP and Normal waves. These upward propagating waves are related to the normal incidence central ray. The NIP-wave originates in the reflection, the normal incidence point (NIP) point central ray ray, and the normal wave is a local approximation of the exploding reflector around the NIP. The CRS traveltime is a second order hyperbolic traveltime approximation for rays in the vicinity of a normal incidence central ray. For the 2D case and a flat measurement line, this is given by (Tygel et al., 1997):

$$t^2(x_m,h)=\left[t_0+\frac{2\sin\beta_0}{v_0}(x_m-x_0)\right]^2+\frac{2t_0\cos^2\beta_0}{v_0}\left[\frac{(x_m-x_0)^2}{R_N}+\frac{h^2}{R_{NIP}}\right] \quad (1)$$

The coordinate $x_m=(x_g+x_s)/2$ is the midpoint and the coordinate $h=(x_g-x_s)/2$ is the half-offset, where the x_s and x_g are the coordinates of the source and receiver position, respectively. The coordinate x_0 and time t_0 are, respectively, the emergence point and the ZO two-way traveltime of the central ray. The parameter v_0 denotes the near surface constant velocity.

Knowing the three kinematic attributes for a certain ZO sample point on a reflection event, the CRS traveltime formula (1) defines a stacking surface, or so-called CRS operator, in the midpoint and half-offset plane. In the CRS stacking method, the seismic amplitudes of the prestack data are summed along the stacking surface to simulate a ZO amplitude. The complete ZO staked section is obtained repeating this procedure for all the possible sample points of the ZO section. To perform the CRS stack and to determine the three CRS-attributes, we use the one-step optimization strategy presented in Garabito et al. (2006b).

CDS-Traveltime

A special case of equation (1) is obtained when the wavefront radius of the Normal wave is assumed to be equal with the wavefront radius of the NIP wave, i.e. $R_{NIP} = R_N$. In this case, the reflection point on the reflector in depth may be considered as a diffraction from the normal incidence point of the central ray. With this assumption, and by restricting to the ZO situation, (i.e. $h = 0$), the ZO common diffraction surface (CDS) traveltime is given by

$$t^2(x_m)=\left[t_0+\frac{2\sin\beta_0}{v_0}(x_m-x_0)\right]^2+\frac{2t_0\cos^2\beta_0}{v_0}\left[\frac{(x_m-x_0)^2}{R_{NIP}}\right] \quad (2)$$

This equation is an approximation of the ZO Kirchhoff type time migration operator. Using ray modeled values of the CRS parameters for the second curved interface of a simple layered model (Garabito et al., 2006), we show in Figure 1 the ZO reflection traveltime curve (blue line), the diffraction curve for a normal incidence reflection point on this second reflector (red line) and the CDS traveltime curve (green line) for the same normal incidence point. This figure confirms the good approximation of the ZO Kirchhoff migration operator by the CDS traveltime function. Due to this property, the CDS operator defined solely by the NIP-wave attributes (β_0, R_{NIP}) was applied in imaging problems, such as approximative pre-stack time migration (Mann et al., 2000), Kichhoff type post-stack depth migration or mapping (Garabito et al., 2006a), macro-model independent migration to zero-offset (Garabito et al., 2009).

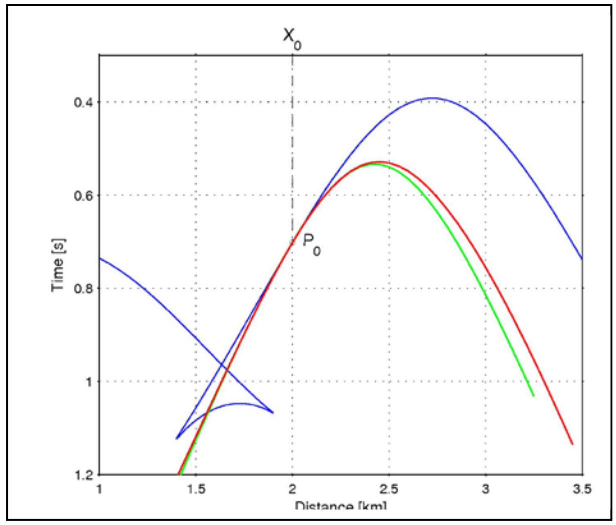

Figure 1. The CDS traveltime curve (green line) and the diffraction traveltime curve (red line) for a normal incidence point on the second reflector. The blue line is the ZO reflection traveltime curve for a second reflector (adapted from Garabito et. al., 2006a).

NUMERICAL RESULTS

Simulation of diffraction events

In this work, with the purpose of determining the velocity model by focussing analysis of diffractions, the CDS traveltime formula (2) will be used to simulate diffraction events at preselected points of the stacked data, at events of known CRS-attributes.

For the numerical tests we use a synthetic model with homogeneous layers, shown in Figure 2. Using ray tracing, we generated 200 shots with 120 traces each, with shot interval of 50 m and the receiver interval of 25 m. The minimum and maximum absolute offsets are 25 m and 1500 m, respectively. The time sample interval of the traces is 4 ms and it was added a low level of random noise to the dataset. To simulate the ZO stacked section and to determine the three CRS-attributes from this synthetic dataset it, we applied the CRS stack algorithm based on the one-step global optimization strategy (Garabito et al., 2006b). Figure 3 is the ZO stacked section obtained by the CRS stack method and, as expected, shows only reflection events. The red points on the reflection events of the Figure 3 were picked using a semiautomatic picking procedure based on the local slope and a coherency threshold.

For these picked points, two CRS-attributes (β_0, R_{NIP}) are used to generate the diffraction events by means of a demigration (i.e. smearing amplitudes along the CDS curve) applied on ZO CRS stacked data (Figure 4). To demonstrate de focalization of the simulated diffractions, we apply on such processed ZO data a Kirchhoff post-stack depth migration using the true velocity model. In (Figure 5) we see that most of the simulated diffractions are nicely collapsed. We can also see how these diffractions moved together with the related reflection events to the correct depth position. The left bow-tie shaped pattern at every imaged diffraction point is merely a consequence of the aperture limitation in the diffraction simulation process. The slightly over-migration of some diffractions, mainly on the top of the second last reflector, might be partly caused by the smoothing of the velocity model, needed for the Kirchhoff migration.

These results show that simulated diffractions from NIP-wave attributes (β_0, R_{NIP}) are useful to estimate the depth velocity model by focusing analysis in a poststack migration process.

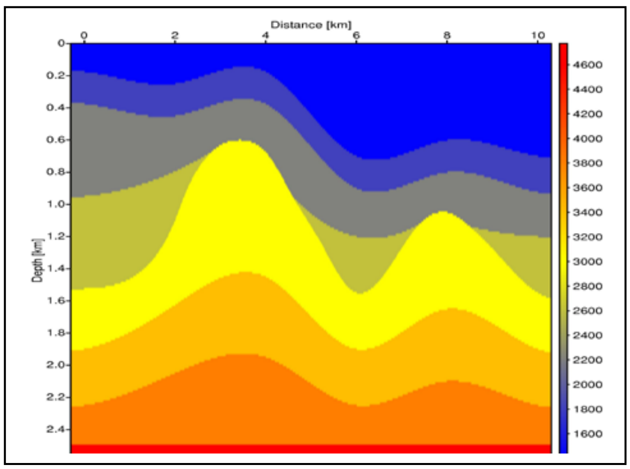

Figure 2. Synthetic layered model with dipping and curved interfaces.

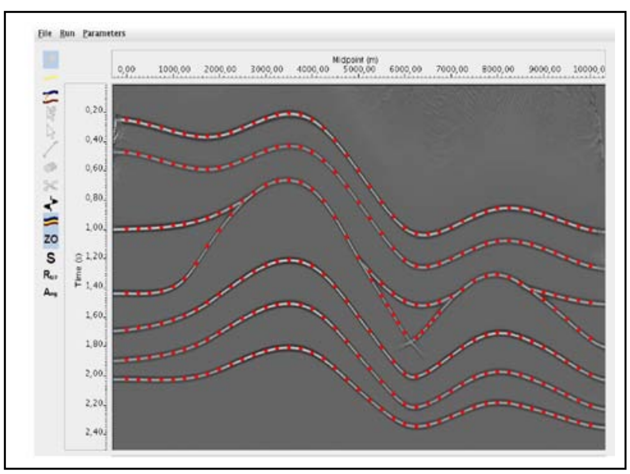

Figure 3. ZO stacked section simulated by CRS stack method. The red points are the picks resulting from semiautomatic picking algorithm.

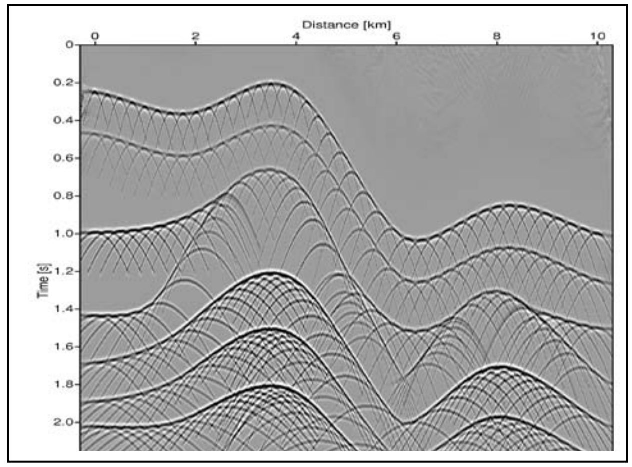

Figure 4. ZO stacked section simulated by CRS stack method including simulated diffractions.

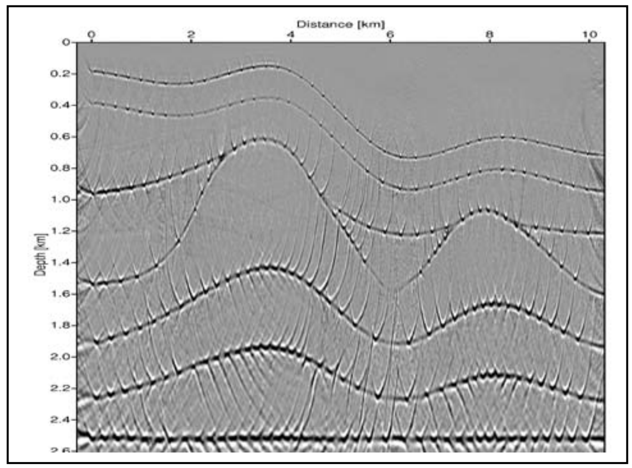

Figure 5. Poststack depth migrated section of the ZO stacked section with simultated diffractions (Figure 4) and using the true velocity mode.

Determination of time velocity model

In the previous section, we have indicated how simulated diffractions from NIP-wave attributes can be used for depth velocity model building in a fast poststack approach. Based on the fact that simulated diffractions are second-order approximations of hypothetical diffraction events, connected to the generating reflections in the real model, they behave also as real diffractions. This property has been demonstrated in depth imaging (Figure 4). Now, we will exploit the focusing property of diffractions in time imaging and show how the same CRS stack with simulated diffractions can be used to determine the time velocity model.

As the measure of focusing diffraction events we use the coherency measure semblance (Neidel and Taner, 1971) and the interactive focusing and defocusing analysis. We use the analytical hyperbolic diffraction traveltime for constant velocity to evaluate the semblance for a given CMP position of the ZO section where the diffraction

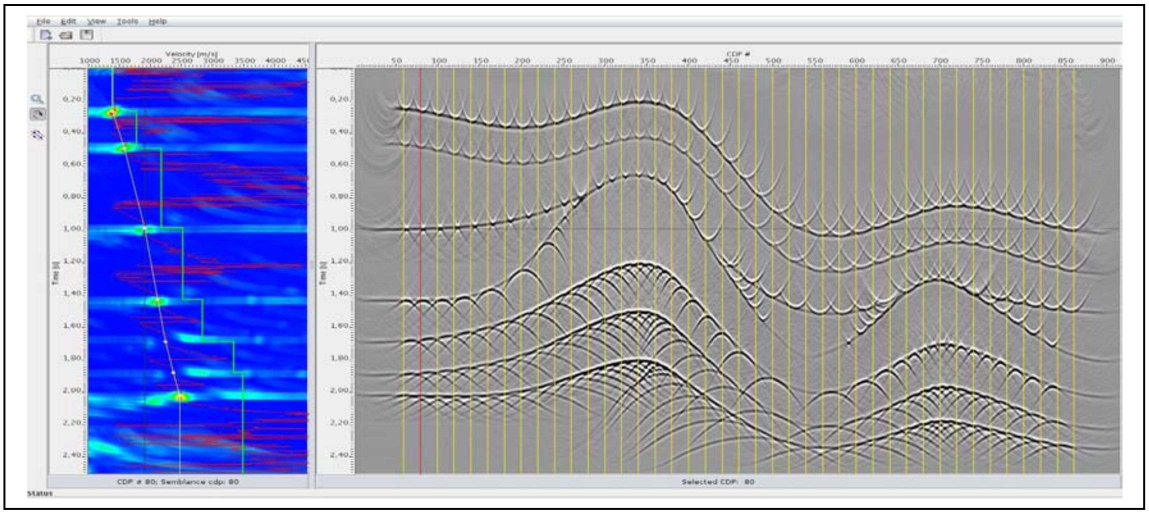

Figure 6. Interactive tool for poststack time velocity analysis by using the velocity spectra (semblance) and the focusing analysis of diffractions.

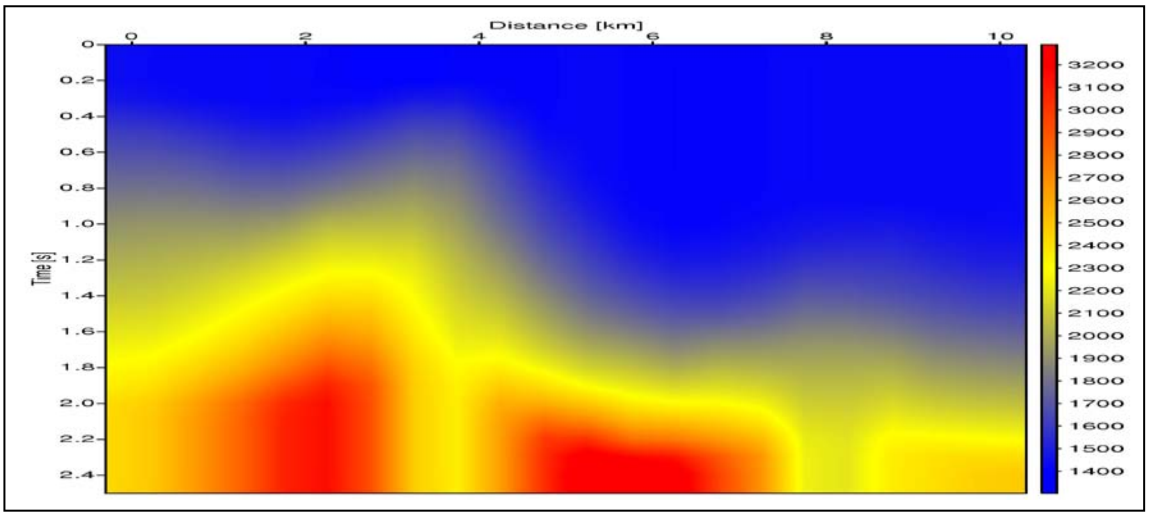

Figure 7. Time velocity model obtained by the poststack interactive velocity analysis based on the diffractions simulated from NIP-wave attributes of the CRS stack method.

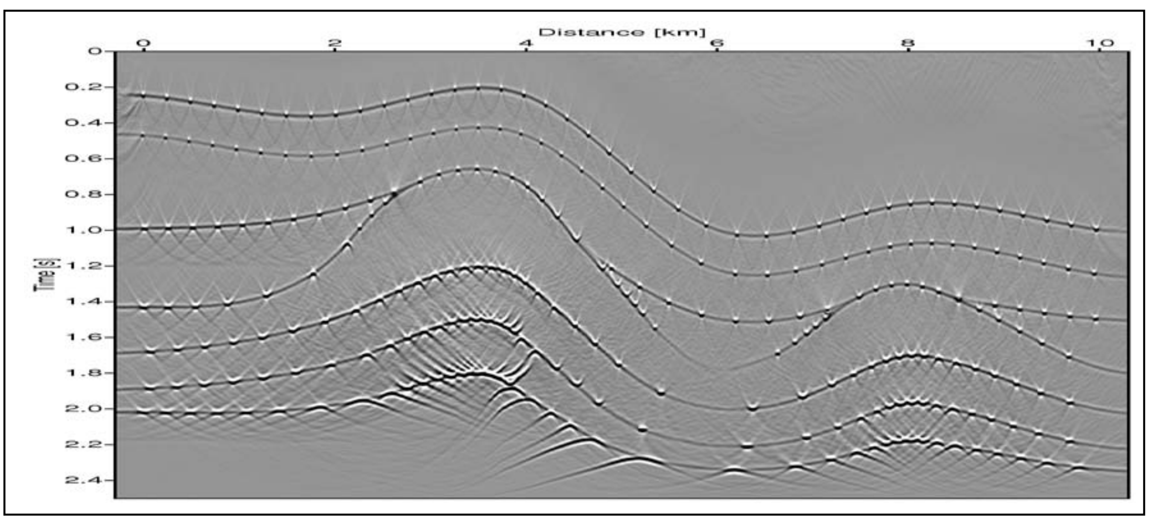

Figure 8. Poststack time migration of the ZO stacked section with simulated diffractions in Figure 4 and using the velocity model in Figure 7.

points are located. An example of the coherency measures for one CMP position is shown in the left panel of the Figure 6. The high semblance values in the velocity spectra panel indicates the best velocity related to the diffraction event. As guide velocity functions we also plot the stacking velocities calculated from the CRS-attributes (in red) in the velocity spectra panels.

For the focusing analysis we apply poststack migrations for a given number of velocities within predefined velocity intervals. Based on the migrated image shown on the right hand side panel of Figure 6 we search interactively for the best focused image and the related velocity for the diffraction event in analysis.

Using the two criteria described before in an interactive manner, we determine the time velocity model shown in Figure 7. This obtained time velocity model was used in a post-stack time migration and applied on the ZO stacked data with simulated diffractions (Figure 4). The migrated result is shown in Figure 8. As expected most of the simulated diffraction events are well focused also in poststack time migration. We presume that the incorrect focusing of the diffractions of the deepest reflector (below the surface location of 2 km and between the locations 4 to 5 km) is due to inaccuracies in the velocity picking process. The chosen velocities in these parts of the section were too high and re-picking in a second round with denser diffractions would be indicated.

Conclusions

We present a stable approach to determine the velocity model from the NIP-wave attributes. The NIP-wave attributes are used in a first step to simulate diffraction responses at predefined points of the CRS stacked data. These simulated diffractions are migrated, in a second step, together with the underlying ZO reflections in a velocity analysis loop. Depending on the migration used in the velocity analysis loop, the resulting velocity model can either be a depth or time velocity model.

The time velocity model building process was demonstrated based on a laterally heterogeneous layered model. Both the coherency measures and the focusing criteria were integrated and analyzed in an interactive tool to facilitate the velocity picking process.

The velocity models obtained from this process are geologically consistent because the diffractions are simulated on preselected points of interpreted reflection events. Both the time and the depth velocity model can be subsequently used in poststack time and depth migration and they are ideally suited as start velocity models for the corresponding prestack imaging processes.

Acknowledgments

The first author thanks CPGeo (Centro Potiguar de Geociências) for kindly supporting this work. The second author thanks PGS (Petroleum Geo-Services, Norway) for the permission to contribute to this development.

References

Biloti, R., Santos, L., and Tygel, M. (2002). Multiparametric traveltime inversion. *Studia Geophysica* et Geodetica, 46: 177-192.

Jäger, R., Mann, J., Höcht, G., and Hubral, P. (2001). Common reflection-surface stack: Image and attributes: *Geophysics*, 66, 97-109.

Duveneck, E. (2004). Velocity model estimation with data-derived wavefront attributes. *Geophysics*, 69: 265-274.

Garabito, G., Cruz, J.C., and F da Luz, S.L. (2006a). Depth mapping of stacked amplitudes along attribute based ZO stacking operator: 76th. Annual Meeting, SEG, Expanded Abstracts, 2629-2632.

Garabito, G., Cruz, J.C., and Hubral, P. (2006b). Application of SA and VFSA global optimization algorithms for search of the 2-D CRS stacking parameters. *Wave Inversion Technology (WIT) Report* (Germany), 24-31.

Garabito, G., Söllner, W., and Cruz J.C., (2009). Macro-model independent migration to zero offset (CRS-MZO), In Expanded Abstract, 71st *EAGE Conference & Exhibition*, Amsterdam, The Netherlands.

Hubral, P. and Krey, T. (1980). Interval velocities from seismic reflection time measurements: Monograph. *Soc. Expl. Geophys.*

Mann, J., Hubral, P., Traub, B., Gerst, A., and Meyer, H. (2000). Macro-model independent approximative prestack time migration. In Expanded Abstracts, 62th Mtg. *Eur. Assoc. Expl. Geophys.*

Mann, J. (2001). Common-reflection-surface stack and conflicting dips. In Extended Abstracs, *71th Annual Internat. Mtg., Expl. Geophys.*

Neidel, N., and Taner, M. (1971). Semblance and other coherency measures for multichannel data. *Geophysics*, 36: 482-497.

Söllner, W. and Yang, W-Y. (2002). Diffraction Response Simulation: A 3D Velocity Inversion Tool. In Expanded Abstracts, *72nd Annual International Meeting, SEG*, 2293-2296.

Tygel, M., Müller, T., Hubral, P., and Schleicher, J. (1997). Eigenwave based multiparameter traveltime expansions. Expanded Abstract of the *67th Annual Internat. Mtg., Soc. Expl. Geophys*.